Detection of Amyloid Plaques Targeted by USPIOs and ARIA Evaluation in a Non-Human Primate Model of Sporadic Cerebral Amyloid Angiopathy (CAA)

Jonathan Leung

Detection of Amyloid Plaques Targeted by USPIOs and ARIA Evaluation in a Non-Human Primate Model of Sporadic Cerebral Amyloid Angiopathy (CAA)

Abstract

Alzheimer's Disease is a neurodegenerative disorder that is one of the most common forms of dementia. While there is still no cure for the disease, early diagnosis of the disorder is important for gauging the efficacy of any treatments. To this end, there have been developments on an MRI method of determining amyloid-β (Aβ) and CAA burden of aged squirrel monkey models of AD using a compound of ultrasmall superparamagnetic iron-oxide nanoparticles, polyethylene glycol, and Aβ-40/42 peptides (USPIO-PEG-Aβ). Analyses of pre- vs. post-injections at various time points suggest that USPIO compounds can cross the blood-brain barrier and accurately bind to Aβ plaques.

Another aim of the study was to determine the efficacy of squirrel monkeys as a model for amyloid-related imaging abnormalities (ARIA) pathology seen in humans. This model can be utilized for determining the efficacy of different immunotherapeutic treatments being tested in non-human primate models for future clinical trials. ARIA evaluation in this model has also been done, helping to better assess the safety of different immunotherapeutic drugs.

The usage of USPIO-PEG-Aβ nanoparticles by medical researchers can help to accurately assess the presence of Alzheimer's disease in patients. While continuing to optimize MRI sequences for better quality images, data that has been obtained suggests that squirrel monkeys show pathology similar to those of human AD patients. Results suggest that the usage of USPIOs combined with white matter hyperintensity analysis of ARIA pathology can be used to effectively gauge the severity of amyloid plaque pathology and non-toxicity in squirrel monkeys.

Detection of Amyloid Plaques Targeted by USPIOs and ARIA Evaluation in a Non-Human Primate Model of Sporadic Cerebral Amyloid Angiopathy (CAA)

1. Introduction

1.1 Rationale

Neuroscientists currently seek a consistent and accurate method for detecting sporadic cerebral amyloid angiopathy (CAA), which is closely linked to Alzheimer's Disease (AD) pathology (Scholtzova, et al., 2015). Prevailing methods of determining the presence of AD in patients is through cognitive tests, which can be inaccurate (Chan et al., 2019). Previous animal models for AD and CAA, such as mouse models, have had difficulty in examining amyloid related imaging abnormalities (ARIA) that aligns with human pathology.

The usage of transgenic mouse models used for past research on AD has progressed, and the need for a model of CAA and AD more closely related to human pathology has risen (Wadghiri et al., 2003). The use of *Saimiri boliviensis*, commonly known as black-capped squirrel monkeys (SQM), as a non-human primate model is effective, since there is a natural generation of CAA pathology. This can be used in future studies to determine the safety and efficacy of immunotherapeutics and assess the possible long-term consequences of ARIA. Current human and animal data shows that CAA, pathology indicative of AD, is more resistant to clearance than parenchymal amyloid and removal may lead to damaging microhemorrhages (Scholtzova et al., 2013). It has also been shown that CAA may be involved in cerebral edema and/or cerebral microhemorrhages (ARIA-E and/or H) in magnetic resonance imaging (MRI) scans of patients receiving amyloid-β (Aβ) immunotherapy (Scholtzova et al., 2018). However, current tests for CAA are invasive and time-consuming.

Therefore, there is a need for a novel method to detect CAA in AD patients. In previous studies of mouse models with ultra-small paramagnetic iron oxide particles bound to polyethylene glycol and Aβ (USPIO-PEG-Aβ), it has been shown that the particles bind to amyloid plaques, suggesting a potential use for labelling CAA pathology (Belaidi & Bush, 2016). As such, my study focused on *Saimiri boliviensis* as a non-human primate model, with a natural generation of CAA pathology similar to that of humans to determine the ability of the USPIO-PEG-Aβ nanoparticles to target and visualize amyloid deposits.

1.2 Background

1.2.1 Alzheimer's Disease

Alzheimer's Disease (AD) is a neurodegenerative disorder acknowledged as one of the most common forms of dementia. It is the sixth leading cause of death in the United States, and the fifth in people aged 65 or older ("Alzheimer's Disease Fact Sheet"). There are an estimated 5.7 million Americans afflicted

with the disease, with this population projected to grow rapidly in the future, reaching an estimated 15 million Americans by 2050 (Korolev, 2014).

Since the characterization of AD by Dr. Alois Alzheimer in 1907, there has been a great deal of effort put into researching the pathology of the disease, especially that of extracellular amyloid plaques made up of aggregates of amyloid beta (Aβ) and intracellular neurofibrillary tangles (NFTs) made up by hyperphosphorylated aggregates of a protein called Tau (Adalbert et al., 2007). While there has been debate on which pathology is the primary cause of AD, the amyloid cascade hypothesis has long dominated the field (Lloret et al., 2019).

The amyloid cascade hypothesis postulates that the extracellular deposition of the Aβ protein is the primary cause of AD and can cause a variety of other pathologies associated with AD. The accumulation of the Aβ protein begins with the cleavage of the amyloid precursor protein (APP), a membrane protein expressed around the synapses of neurons. The accumulation of Aβ in the brain leads to amyloid plaques that can cause cerebral amyloid angiopathy (CAA) pathology.

Cleavage of the APP can occur in two pathways: non-amyloidogenic, referring to non-aggregates, and amyloidogenic, which can lead to pathogenic aggregating types (Zhao & Lukiw, 2015). While both pathways do occur in normal human biology, the amyloidogenic pathway has been suggested to lead to the pathogenesis of AD. As the APP metabolism transforms during the course of AD development, the pathways generally shift from non-amyloidogenic to amyloidogenic, resulting in accumulation of Aβ40 and Aβ42, the more toxic Aβ protein due to its ability to aggregate (Wang et al., 2010). This cerebrovascular deposition of Aβ is described as CAA, commonly used to gauge AD pathology.

1.2.2 Cerebral Amyloid Angiopathy (CAA)

CAA has been hypothesized to be the result of the increased failure of the brain to eliminate aberrant Aβ that comes with age (Scholtzova et al., 2014). In rare cases, CAA can also develop genetically. There are three main methods that the brain typically eliminates Aβ: enzymatic degradation in parenchyma, direct absorption into the blood via lipoprotein receptor-related protein, and perivascular drainage with other solutes, which is much slower than the other forms of elimination and is where the CAA typically occurs. CAA is thought to be the result of the increased failure of the brain to eliminate aberrant Aβ that comes with age (Scholtzova et al., 2013).

Despite the known pathologies of AD, diagnosis in patients is still difficult. Aside from the postmortem analysis of the brain to determine presence of NFTs and Aβ plaques, current diagnosis of AD involves cognitive tests, neurological exams, genetic screening for certain at-risk genes, and structural brain imaging to see any potential damage in the form of atrophy, fluid buildup or evidence of a stroke.

While physicians can determine if a patient has dementia, determining if the neurodegeneration is specifically AD is more intensive and difficult to ascertain. With new advances in magnetic resonance imaging, there has been interest in the development of contrast agents that can cross the blood-brain barrier (BBB) and label Aβ plaques that can be viewed in-vivo. In the new world primate, *Saimiri boliviensis*, natural generation of CAA pathology does occur (Genovese et al., 2019).

1.2.3 Non-Human Primate Models, *Saimiri boliviensis*

While there is still not yet a cure for the disease, early diagnosis is a critical factor in assessing the efficacy of any treatments. On account of this, there have been developments of a novel MRI method of determining Aβ burden within the brain of a non-human primate model. This project utilized the females of the primate species, *Saimiri boliviensis*, commonly known as squirrel monkeys (SQM). In new-world monkeys such as *Saimiri boliviensis*, previous experiments have indicated the natural development of Aβ plaques after the age of 15 predominantly in the form of CAA. However, the other major pathology that is used to characterize AD, Tau tangles, is absent from SQM models (Adalbert et al., 2007). As such, the non-human primate model used, in this study, focused on the amyloid cascade hypothesis and was used to model CAA and determine if the compounds used in the study were indeed effective. In addition, the APP gene in SQMs has a 95% homology to the human gene, making the model optimal to study (Scholtzova et al., 2016). Other than the improved visualization of Aβ plaques in a non-human primate model, there was also hope to show that SQM models exhibited amyloid-related imaging abnormalities. Prominence of CAA in SQMs also aid in determining ARIA-related pathology that may develop.

For the first time in a non-human primate model, there was advocation for the utility of the novel MRI methodology, bi-functional ultra-small superparamagnetic iron oxide (USPIO) nanoparticles coupled to polyethylene glycol (PEG) and Aβ 40/42, to identify CAA burden and document therapeutic efficacy of various immunotherapies (Pansieri et al., 2018). The potential usage of these nanoparticles to evaluate the CAA pathology in human or non-human primate models may be extremely beneficial for the assessment of immunotherapeutic medicines, as well as assess the presence of AD – like symptoms in patients with dementia.

Using the non-human primate model of *Saimiri boliviensis* (SQM), commonly known as the black-capped squirrel monkey, it was possible to model the Aβ plaque pathology in aged SQM that naturally develop CAA and amyloid pathology starting around the age of 15 (Scholtzova et al., 2015).

1.2.4 Previous Models of Alzheimer's Disease and Iron Oxide Nanoparticles

In previous studies on methods of labelling amyloid plaques *in vivo*, there have been other types of methods of bypassing the blood-brain barrier (BBB). Previously, a mannitol injection was used to

temporarily open up the BBB so that the injection of ultra-small paramagnetic iron-oxide (USPIO) nanoparticles coupled to Aβ peptides could correctly reach and label the plaques (Scholtzova et al., 2008). While the results did indicate that there was correct labelling, the mannitol injection itself was invasive, and not suitable. As a subsequent experiment, bi-functional USPIOs coupled to Aβ peptides and a polyethylene glycol compound was tested for efficacy (USPIO-PEG-Aβ). It has been shown that polyethylene glycol gives permeability through the BBB by increasing the half-life of plasma and inhibiting its intake by the reticuloendothelial system, making it a beneficial compound to use for nanoparticles reaching the brain (Genovese et al., 2019).

Previous research with the study of multiple mouse models of AD had also been done in the lab. The BBB is made of endothelial cells that line cerebral micro-vessels that have an integral role in maintaining a suitable environment for neurological signaling. It also acts as a physical barrier due to the tight junctions that the cells have with each other and only allows very specific transcellular transport across. While previous compounds, such as the Pittsburgh compound developed by the University of Pittsburgh did show early success, usage of positron emission topography (PET) scans did not have high enough resolution to visualize individual amyloid plaques or assess density of plaques (Gurol et al., 2016). As such, it has been determined that usage of USPIO-PEG-Aβ nanoparticles should be tested in an advanced model of amyloid. In addition, MRIs have proven to be better for visualization than PET scans, as it is more detailed.

With the success in mouse models that USPIO-PEG-Aβ studies have had in correctly labeling amyloid plaques, the need arises for a more similar model of human Alzheimer's disease and CAA pathology. To this end, the utilization of SQM models was needed for comparison to human models, which could eventually be used for tests in clinical trials.

1.2.5 Aβ and CAA in SQM Models

To determine the Aβ burden in these SQMs the usage of a compound of ultra-small superparamagnetic iron-oxide nanoparticles (USPIO), polyethylene glycol, and Aβ-40 or Aβ-42 peptides was employed. In previous tests done with this novel compound, there has been usage of bi-functional USPIO nanoparticles coupled to both the Aβ peptide, as well as polyethylene glycol which had been previously shown to allow some permeability through the BBB by extending the plasma half-life, in addition to inhibiting uptake of the compound via the lymphatic system. With the usage of T2* analysis and cross reference with histological staining for Aβ plaques, it has been shown that plaques were labeled and visible on in-vivo MRI scans (Ruff et al., 2017).

With there being great interest in the ability to quantify the brain in-vivo, MRI techniques are being developed. While many techniques have been proposed, there has never been a chemical validation to assess

the amount of iron normally found in the brain. However, there have been previous studies that demonstrated that high amounts of iron in the body may cause susceptibility changes and microscopic field gradients.

Iron plays a critical role in many normal biological functions; if not properly regulated, it can cause many neurological disorders, including AD (Belaidi & Bush). In a study of APP, there has been evidence that there was ferroxidase activity that helped to metabolize and remove iron. Furthermore, Zn^{2+}, an ion that accumulates with Aβ plaques may block activity of the APP and lead to increased iron burden. The iron burden corresponding to different neurodegenerative disorders indicates that it is a good biomarker that can be used as a monitor of the severity of disease. It is important to have a quick and non-invasive method to track the disease in patients with such conditions. In the SQM models that are being used, the presence of human-analogous CAA and Aβ plaques suggest that aged SQMs are a good model for testing AD treatments prior to clinical trials, that are also able to be imaged to track ARIA-related pathologies. Although the plaques are not as large as in human or mouse AD models, relative to brain size, the hope is to see an increase in total iron burden when injected with the USPIO-Aβ-PEG compound.

Evidently, the focus of this project was on the validation of USPIO-Aβ-PEG nanoparticles for visualization of amyloidosis and CAA that is correlative to AD pathology. This was done in addition to the evaluation of non-toxicity of the USPIO-Aβ-PEG nanoparticles with the usage of ARIA-E and immunohistochemical analyses. Usage of new-world SQM models for their natural generation of CAA was also important for determining a pre-clinical model for AD patients and immunotherapies.

2. Methodology and Materials

**All methods were conducted by Author unless otherwise stated*

2.1 Animals (all work with animal models were done by mentor)

Saimiri boliviensis, commonly known as squirrel monkeys (SQMs), were randomly selected from the Squirrel Monkey Breeding Facility (SMBRR) at the Michale E. Keeling Center for Comparative Medicine and Research at the University of Texas, MD Anderson Cancer Center. The SMBRR, located in Bastrop, Texas, is the largest SQM breeding facility in the world. In the process of conducting this study, the Animal Welfare Act, PHS Animal Welfare Policy, and the NIH Guide for Care and Use of Laboratory Animals were closely followed.

However, I had no direct interaction with the living SQMs done at the research in NYU Langone where I worked. All tissue samples and materials were obtained from the facilities in Bastrop, Texas which I did not have any direct contact with the living SQMs. All injections and scans were performed by my mentor and other laboratories in Houston, Texas.

Squirrel monkeys are a natural model of CAA, in which their Aβ sequence matches that of humans, making them an ideal model to test the MRI contrast agents used in this project to determine if the model is suitable for determining ARIA-related pathologies (Scholtzova et al., 2018). Small new world primates have a maximum lifespan averaging around 26 years of age. As squirrel monkeys naturally develop amyloid plaques starting around the age of 15, in which CAA is more prominent than parenchymal amyloid plaques, no animals younger than 19 years of age were used to ensure that all of the monkeys in the study cohort had significant pathology.

Squirrel monkeys were placed into cohorts of 4 aged monkeys between the ages of 19 to 21 years old. Monkeys were scanned at intervals that would not cause any harm, at various time points of 12 hours, 24 hours, 36 hours, 48 hours, and 6 weeks after I.V. injection of the target nanoparticle to evaluate optimal imaging times for maximum plaque detection and to determine time needed for clearance of USPIO-PEG-Aβ nanoparticles. I.V. injections of target nanoparticles were done in Texas, and I did not have any contact or handling with the monkeys.

2.2 MRI Contrast Agents (prepared by an external facility)

Aβ1-40 and Aβ1-42 (both strongly correlative with AD pathology) were both synthesized at the W.M. Keck Facility at Yale University (New Haven, CT). Synthesis, purification, and sequence verification were performed in a step process, in which Aβ1-40 was obtained in dissolved trifluoroacetic acid salts and diluted with water to 16.7% of dimethyl sulfoxide (DMSO) (Genovese et al., 2019).

The ultra-small superparamagnetic iron oxide (USPIO) nanoparticles (made with a concentration of 10 mg Fe/ml by Ocean Nanotech) were linked to Aβ1-42, or Aβ1-40, and PEG using standard EDC/NHS.

Aβ peptides are known to have high affinity binding to each other, in particular with single monomer Aβ to deposited, aggregated Aβ. Coating USPIO nanoparticles with monomeric Aβ1-42 or Aβ1-40 is expected to target the particles to amyloid plaques, as evident in prior publications done with the USPIO-PEG-Aβ (Punia et al., 2019). The usage of a polyethylene glycol has shown to be able to bypass the BBB, and when coupled to a bi-function iron oxide nanoparticle with Aβ peptides could bind to the appropriate CAA amyloid plaques located in the brain (**Figure 1**).

Animals were injected I.V. via the femoral vein with 4ml of targeted nanoparticles dissolved in 5% Dextrose via a computer-controlled syringe pump (Harvard Apparatus, rate: 0.25ml/min.; duration 16min), using a dose within the range prescribed in human studies (3.5mg/kg body weight) (Genovese et al., 2019). Injections done with the USPIO-PEG-Aβ nanoparticles were not performed by me and were instead performed by qualified scientists and researchers at the SMBRR facility.

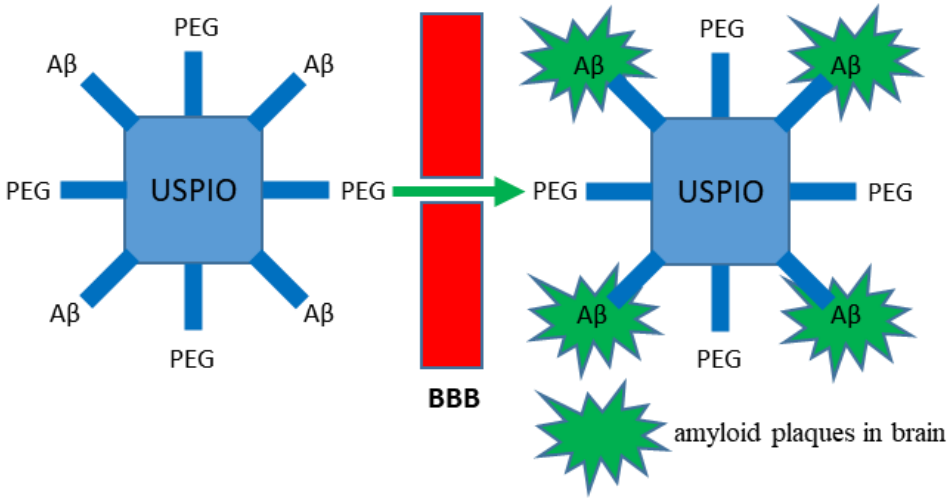

Figure 1.
Polyethylene glycol (PEG) allows for the bi-function nanoparticle to bypass the blood-brain barrier (BBB), permitting specific Aβ peptides to bind to the amyloid plaques. Once bypassing the BBB, the bi-functional iron oxide nanoparticle shows up on different MRI scans as bright spots, which allows for analysis and confirmation of the presence of microhemorrhaging in the brain caused by cerebral amyloid angiopathy. (Author)

2.3 *In vivo* MRI Brain Imaging (performed by external laboratory)

Initial *in vivo* MRI experiments were designed to test toxicity and utility of the novel MRI compound of bi-functional ultra-small superparamagnetic iron oxide nanoparticles (USPIO) bound to polyethylene glycol and Aβ40/42 (USPIO-PEG-Aβ) to determine Aβ plaques/deposits and to confirm CAA burden in aged SQMs as a vehicular group (Scholtzova et al., 2015). For direct work with handling the SQMs, I did not have physical contact with the living SQM, instead working with the brain tissue collected by my mentor.

For USPIO-PEG-Aβ compound scans, a T2*-weighted image was acquired using a multigradient echo (MGE) sequence [MGE; TE=2.96ms ES=4ms, 8 echoes, TR=41ms, FA ~13deg., time=45min, 3 repetitions] at spatial isotropic resolution (200μm).

In vivo multiple – readout gradient echoes (MGE), fluid-attenuated inversion recovery sequences (FLAIR), and rapid acquisition with refocused echo sequences (RARE) scans were done at the SMBRR facility where the SQMs were housed. These *in vivo* sequences were sent in digital imaging and communications in medicine (DICOM) file format. Scans were then received and analyzed by me for their respective studies or markers, such as white matter hyperintensities for CAA or bright spots indicative of iron oxide nanoparticles.

2.4 Generation of R2* Maps and Region of Interest Based Analysis

R2* maps were made from 3D MRI images using a software called FireVoxel, developed by the NYU Langone Health faculty of the Department of Radiology, Artem Mikheev and Henry Rusinek. The program allows uploading of 3D DICOM T2*-weighted images and generates an R2* (1/T2*) map based off of the original image that can be color coded or in grayscale. On the MRI scans, T2* maps would show with inverse coloring, flipping analysis that needed to be done (Weissleder et al., 1990). On R2* maps, areas of the brain affected by amyloid plaques show up as bright areas, whereas the inverse scan of T2* show plaques as dark areas. R2* measurements are considered to be linearly related to the iron content in the brain, allowing for accurate analysis of SQM scans.

Regions of interest (ROIs) were analyzed using ImageJ on brain regions known to display the presence of Aβ plaques (Genovese et al., 2019). Subsequent to coregistration of SQM images using FireVoxel, specific ROIs were marked on cortical regions and measured for the average signal intensity. ROI analysis was done for 5 slices per region, where the 5 slices were separated by 3 slices.

Due to the injection of USPIO-PEG-Aβ, iron-rich areas of the brain would show as darker regions, indicative of the related CAA pathology that causes microhemorrhaging in the brain. However, because R2* maps were being utilized, iron-rich areas of the brain would show as lighter/hyperintense regions, correlative to higher averaged values within the specific ROI being analyzed. GraphPad Prism was used for statistical analysis.

2.5 Histology

Brain tissue obtained from the appropriate squirrel monkey cohorts were sent to the lab for the larger immunotherapeutic study. Of the three squirrel monkeys that were allocated for the USPIO-PEG-Aβ study, one was sacrificed for histological comparisons. All cutting and paraffinization of the brain was done by my mentor and the appropriate faculty, of which I had no part working with the squirrel monkey tissue prior to mounting on the slide. Histological stains were then appropriately chosen according to markers that needed to be tested. Examples include GFAP, which stains for astrocyte locations and 6E10, an anti-amyloid beta antibody. These markers could then be used to compare

whether the regions marker on MRI scans were accurate and aligned to the histological markers that showed up after immunohistochemical stains. All sections were 8 microns thick and cut by mentor and were used for the immunohistochemical procedures. A wide range of histological processes were utilized, of which I had optimized and tested for the usage on squirrel monkey brain tissue, developing protocols that were suitable for comparison to the various MRI scans performed.

2.5.1 Perl Prussian Blue Stains

Perl Prussian Blue Stains were utilized for the visualization of microhemorrhaging in the brain. Perl Prussian Blue Stains use a ferrocyanide solution, specifically binding to iron deposits left by hemorrhages in the brain. Using a combined solution of hydrochloric acid and potassium ferrocyanide, slides were run under a heated protocol. After incubation in the combined ferrocyanide and hydrochloric acid solution, slides were counterstained with nuclear fast red stains to provide a red contrast to the blue stains that are left behind. Usage of this type of staining was for confirmation of CAA in the brain. After the Perl stain and counterstain with nuclear fast red for the nuclei of neurons, slides were cover slipped and left to dry overnight. Analysis and photos were done using Bioquant imaging systems and a microscope camera.

I also did optimization of a variety of Perl stains, including no-heat and heat–intensive one-day staining protocols. I tested different concentrations of hydrochloric acid and ferrocyanide solutions, gauging changes in protocols that needed to be made after each stain. If stains were too light or had too much background, cleaning of the slides under tap and distilled water was tested. The general consensus for the best Perl SQM histology done was with the usage of a heat-intensive protocol using 20% HCl and 10% potassium ferrocyanide solution microwaved at high power for 30 seconds, then letting sit for 10 minutes to cool down in the fume hood. Slides were then washed under warm tap water for 10 minutes. Slides were placed for a 1-minute nuclear fast red stain to give contrast to the blue-stained microhemorrhages and for comparison to the location of neurons. Slides were then dehydrated using an ascending grade of ethanol and xylenes and coverslipped with a coverslip glue.

The necessary solution precautions were also followed, including the proper disposal of the chemicals. Photos and analysis were done afterwards for confirmation of CAA in the brain.

2.5.2 Diaminobenzidine (DAB) Stains

Diaminobenzidine (DAB) stains were utilized in a variety of different histological stains. DAB stains leave a dark black-purple stain on the specific marker they bind to. Most DAB-based stains take two days to run. DAB stains specifically run for this project included GFAP to stain astrocytes and 6E10/4G8 for amyloid. DAB staining protocols encompass a two-day staining

process, in which slides are stained to determine the severity of AD pathology. Primary and secondary antibodies specific to the protein that is being stained were utilized after regular deparaffinization of sections. During the immunohistochemical staining procedures, the regular washing buffer used was 1x – phosphate-buffered saline (PBS) was used for washes in between incubation times. This washing buffer was used in between primary antibody, secondary antibody, and blocking incubations. This stain type of stain was done to help confirm the presence of CAA pathology in the brain, which further exact matching may be needed with corresponding markers and proteins. I continued to develop different DAB stains for the specific aged SQM model that we were working with. Stains done with DAB included 6E10/4G8 and GFAP, which allowed for better visualization of the ARIA-E exhibited in MRI scans. This would aid in the validation of the USPIO-PEG-Aβ compound as a non-toxic novel MRI method for accurately and more easily labelling CAA pathology that is indicative of AD pathology.

The necessary precautions with dealing with the solution were also followed, including the proper disposal of the chemicals. Photos and analysis were done afterwards for confirmation of CAA in the brain. Matching of immunohistochemical stains to ARIA-E regions of interest was also done to further assess toxicity of contrast compound injections utilized.

2.5.3 Luxol Fast Blue Stains

The usage of Luxol Fast Blue Stains were used to stain the myelination in the brain. Being able to compare the visualization of myelin helps to show areas of demyelination in the brain. Luxol Fast Blue Stains utilize a copper phthalocyanine dye soluble in ethanol which binds to bases found in lipoproteins located on myelin sheaths (Dong et al., 2018). Once stained, myelin fibers appear as blue and nerve cells appear as purple. Tissue sections are left in the dye overnight and then differentiated using a lithium carbonate solution. Normal cover-slipping with an ascending grade of ethanol and xylene occurs to dehydrate the slide, which is then covered using a coverslip glue. Slides were also viewed under the microscope for confirmation of myelin disruption in CAA affected regions to confirm analysis done with R2* region of interest-based analysis. CAA can also contribute to the development of ARIA, which this histology was done to pathologically characterize the MRI scans done.

3.0 Results and Discussion

**Statistical analysis established at $\alpha = 0.05$ for significance*

3.1 Region of Interest-based Analysis of USPIO-Aβ-PEG Compounds

A total of three SQMs were utilized in my project, with two being injected with the USPIO compound, and the other being injected with Feraheme, another type of iron-based compound used to treat iron deficiency anemia, as a control. SQMs were imaged prior to injection for baseline values, and again at various timepoints post-injection. For this project, the two SQMs that were injected with the USPIO-PEG-Aβ compound were 2650 and 2648. The monkey that did not receive any treatment was 2823 and acted as a control. The brain maps shown in **Figure 2** is from 2650. The R2* map calculations were repeated 3 times for each time point, with both 2648 and 2650 being analyzed.

Individual amyloid plaques were not visualized, however, increases in hypointense regions of the brain were tracked. Pre- and post- injection brain images (pre, 12 hr, 36 hr, 6 wk post) with darkening effects were recognized. Darkening effects noticed in the brain after injection were noticed to correspond to Aβ deposits and microhemorrhages. **Figure 2** shows these darkening effects located in the gray matter regions of the SQM midbrain. Orange arrows on the R2* brain maps and regular MGE scans show areas where its visually clear that there were hypointense enhancements due to the USPIO-PEG-Aβ contrast injection. MGE slices were all aligned to show the change in R2* values as a result of USPIO-PEG-Aβ nanoparticle injections in regions that typically have Aβ plaques and CAA.

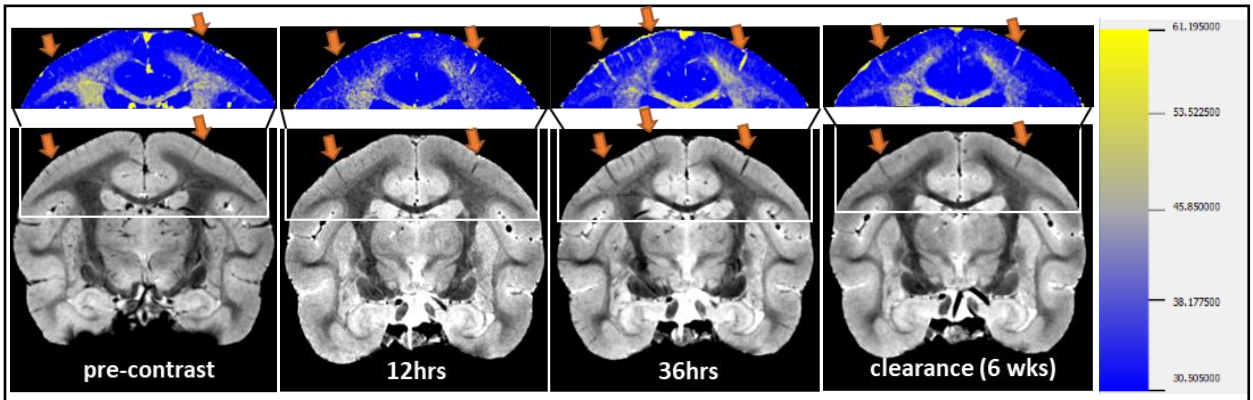

Figure 2.
Figure 2 shows the pre- and post- contrast injection brain images of the timepoints from pre-contrast, 12 hr post, 36 hr post, and 6 weeks post-contrast. The darkening effects of Aβ deposits and microhemorrhages are indicated by the arrows. The R2* brain maps of the pre- and post- injection MRI scans were created with the help of the FireVoxel parametric map tool. Region-of-interest (ROI) based quantitative R2* analysis was done to determine CAA pathology in the aged SQM blocks. There was significant increase of R2* values of the 36-hr timepoint post-contrast injection. *p*-values were calculated and evidently showed increase in R2* values (Author)

R2* brain maps were developed using FireVoxel parametric map tools, and regions of interest (ROI) were developed to do quantitative analysis. When comparing the 36 hr post-contrast injection to the 12 hr post-contrast injection, there was a significant increase of R2* values. Areas of the region where ROI-based

analysis was performed included the prefrontal cortex (PFC), fronto-parietal cortex (FPC), temporal cortex (TC), and hippocampus (HIPP).

There was no evidence of any detrimental or harmful effects observed during the MRI study with the elderly monkeys, indicating the safety of this novel MRI contrast methodology. There was an increase in R2* value in regions where Aβ pathology is expected, including the prefrontal cortex, fronto-parietal cortex, and the occipital cortex, which were all included in ROI analyses done. ROI-based analysis was performed on each repetition of the R2* maps individually. The averages of 3 repetitions of each region for both 2650 and 2648 were calculated. As evident in **Table 1**, there was a significant increase in the averages for R2* values from pre-injection to the 36 hr timepoints.

Table 1.
Significant increases of R2* values were observed at the 36hrs post-contrast injection timepoint compared to the 12hrs post-contrast injection timepoint in all analyzed brain regions. Subsequent analysis revealed significant decreases of R2* count values 6 weeks post-injection when compared to 36 hr post-contrast injections in all brain regions. (Author)

Aged SQM (19-21 years old)	Prefrontal Cortex	Fronto-Parietal Cortex	Temporal Cortex	Hippocampus
pre-injection MRI scan (baseline)	25.55±3.16(12.36)	29.42±3.55(12.07)	27.29±4.27(15.65)	25.60±4.14(16.19)
12hr post-injection MRI scan	25.74±2.82(10.97)	29.14±2.80(9.60)	26.68±2.96(11.11)	23.86±3.00(12.59)
24hr post-injection MRI scan	25.98±2.69(10.36)	30.45±3.13(10.29)	28.39±3.76(13.24)	26.10±3.68(14.12)
36hr post-injection MRI scan	26.83±2.69(10.01)	30.58±3.48(11.39)	28.51±3.77(13.21)	25.59±3.39(13.24)
48hr post-injection MRI scan	26.60±2.45(9.21)	30.37±2.67(8.78)	28.45±2.91(10.23)	26.61±4.18(15.71)
6wk post-injection MRI scan (clearance)	24.78±2.86(11.53)	28.96±3.37(11.65)	27.35±3.93(14.36)	24.76±3.31(13.35)

The *p*-values of the data were also calculated using Microsoft Excel. In **Table 2**, the *p*-values were calculated for comparisons between each time point to better determine whether the USPIO-PEG-Aβ nanoparticles were the cause of R2* value changes. For each region, 5 slices were done, with each slice being separated by 3 slices on the MGE scans. Repeating it 3 times for each of the 4 regions per timepoint, this would be a total of 360 slices that were analyzed with individual ROIs placed on related areas.

Note that the *p*-values of the HIPP when compared to the other cortices were higher. This was mainly due to the region having the least amount of amyloid burden. It has also been shown that the HIPP in general has lower pathology.

Using the data gathered from **Table 1** and **Table 2**, graphs were made using GraphPad Prism. Considering the *p*-values also included, it is evident that there is some sort of causal relationship between the R2* values suggesting hyperintensities and the USPIO-PEG-Aβ nanoparticle contrast injection. It is evident that the p-values calculated are significant with the baseline of $p < 0.05$ for significance. Especially when comparing the 12hr vs. 36 hr post-contrast injection timepoints, statistical significance is established.

Table 2.
p – values of the R2* values were calculated using Microsoft Excel. Data obtained, when compared to the establishment of $\alpha = 0.05$ for significance**,** suggests that the usage of USPIO-PEG-Aβ nanoparticles for labelling amyloid plaques has an effect. Due to the chemical composition of the nanoparticle, it is probable that it is correctly labelling Aβ. (Author)

Aged SQM (19-21 years old)	Prefrontal Cortex	Fronto-Parietal Cortex	Temporal Cortex	Hippocampus
***p*-value (pre-*vs*-36hrs)**	0.015*	0.109	0.064	0.995
***p*-value (12hrs-*vs*-36hrs)**	**0.030***	**0.039***	**0.022***	**0.009****
***p*-value (36 hrs-*vs*-clearance)**	0.029*	0.0193*	0.042*	0.047*
***p*-value (pre-*vs*-clearance)**	0.098	0.362	0.912	0.166

In **Figure 3**, it is clear that there is a drastic and significant increase of R2* values from the pre- to 36 hr post-injection timepoints. There is an evident pattern of R2* values increasing to a maximum at around 36 hrs, implying that for future studies, the timepoint to best view USPIO-PEG-Aβ binding is 36 hrs post-injection. Looking at the error bars provided in the graph by calculating p-values, the R2* value changes from pre- to post- contrast is most probably caused by the USPIO compound which labels CAA.

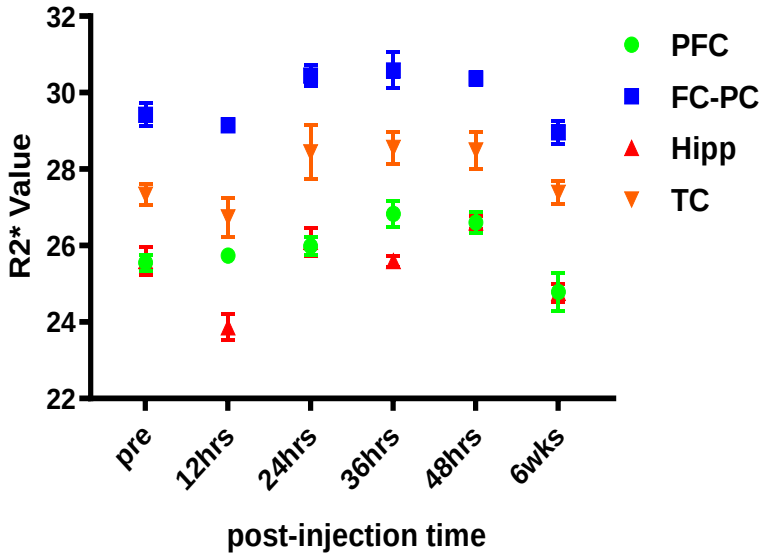

Figure 3.
The *p* – values of USPIO-PEG-Aβ nanoparticles indicates that there is significance, especially between the 12 hr and 36 hr timepoints. There is a visible positive pattern of an increase in R2* values as a result of the USPIO-PEG-Aβ injection. Given chemical composition of the compound, it suggests that the amyloid plaques are being bound to. (Author)

The clearance timepoint of 6wks post-injection R2* values were also very similar to the pre-contrast injection values, allowing for the USPIO-PEG-Aβ to clear the system. This also suggests that the injection compound is non-toxic and non-permanent. Because of the labelling that the USPIO-PEG-Aβ compound has in the brain, the amyloid plaques that are labelled highlight the CAA that is present in aged SQM models.

3.2 Validation of Amyloid-Related Imaging Abnormalities in *Saimiri boliviensis*

The examination for the presence of hyperintense regions on T2-weighted images was needed, as it was shown to be linked to the presence of parenchymal vasogenic edema, sulcal effusions, and subcortical white matter hyperintensity (WMH) patterns. In order to assess whether the usage of USPIO-PEG-Aβ nanoparticles was effective in labelling amyloid plaques, it was necessary to also assess whether the models of *Saimiri boliviensis* (SQMs) even had pathologies related to AD, as well as amyloid burden. As such, it was important to assess whether the aged SQM had amyloid plaques/burden, which follows the amyloid cascade hypothesis, which is considered to be the prevailing pathology causal of AD. This was done with the validation of amyloid-related imaging abnormalities (ARIA) with histology, which was used to determine whether USPIO-PEG-Aβ nanoparticles were non-toxic. The aged SQM model used for **Figures 4 and 5** were from SQM 2238, a 25-year-old female SQM, which was sacrificed for another part of the larger ongoing immunotherapeutic study for AD.

T2-weighted images and data were collected using multi-slice turbo-spin-echo sequences performed after a fluid-attenuated inversion recovery sequence (FLAIR) preparation. Amyloid-related imaging abnormalities such as the T2 – weighted asymmetric signal hyperintensities were detected using white matter hyperintensity analysis. This was primarily detected in the parieto-occipital white matter in the aged female SQM model. ARIA-E, a subset of ARIA that refers to cerebral edema, showed abnormalities that extended along the rostro-caudal axis for several mm, leading to an asymmetrical brain pattern that is correlative to CAA. **Figures 4A, 4B, 4C, and 4D** show the white matter signal hyperintensities at 2 different coronal levels, marked by the red arrows.

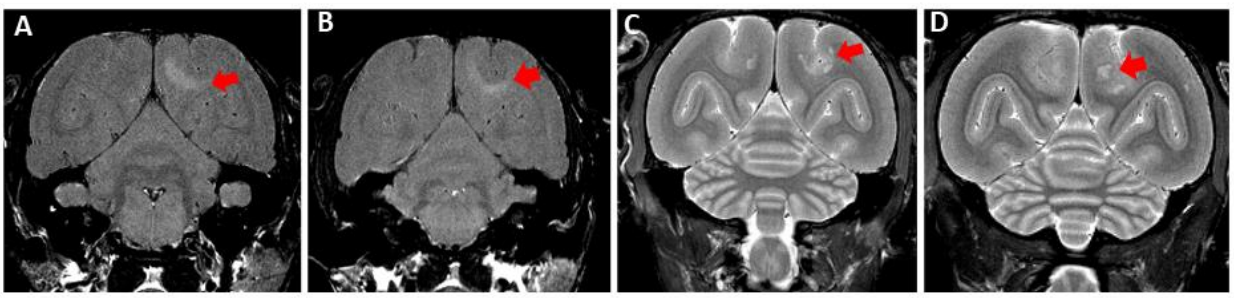

Figure 4A, 4B, 4C, 4D.
The bright white spots that indicate by the red arrows are white matter hyperintensities. The presence of this pathology and asymmetric signal hyperintensities indicate that there is the presence of ARIA-E located in the cerebral edema of the aged SQM model. (Author)

Usage of formalin-fixed, paraffin-embedded coronal sections were analyzed to the characterize histopathological features of specific regions of the aged SQM exhibiting signal abnormalities by MRI.

Usage of different immunohistochemical procedures for markers and proteins such as amyloid, microglia, astrocytes, and myelin was necessary to accurately determine if an SQM had the pathology indicative of CAA and/or possible predictors of CAA.

The disruption of myelin sheath integrity was examined through stains using Luxol Fast Blue (**Figure 5A**). Severe microgliosis, which is the death of microglia, was perceived throughout the whole of the affected brain regions with the use of ionized calcium binding adaptor molecule 1 (Iba1) protein markers (**Figure 5B**). ARIA-E regions were surrounded with abundant astrogliosis marked by glial fibrillary acidic protein (GFAP) (**Figure 5C**). In addition, the presence of CAA and mostly diffused parenchymal plaques was confirmed with 6E10/4G8 immunohistochemistry (**Figure 5D**). The regions displayed in **Figures 5A, 5B, 5C, and 5D** match up to the regions marked by the red arrows in **Figures 4A, 4B, 4C, and 4D**. Being able to confirm that the causal agents of the white matter hyperintensities were amyloid-β further affirms that the ARIA-E noticed in the MRI scans of the aged SQM models were caused by CAA. Note that the amyloid-β stained by the 6E10/4G8 in **Figure 5D** has a seemingly different pattern than the marker stains in **Figures 5A, 5B, and 5C** because amyloid-β is not present in white matter. Instead, the amyloid-β present surrounds the white matter in the gray matter regions, essentially causing microhemorrhages and neurodegenerative pathologies.

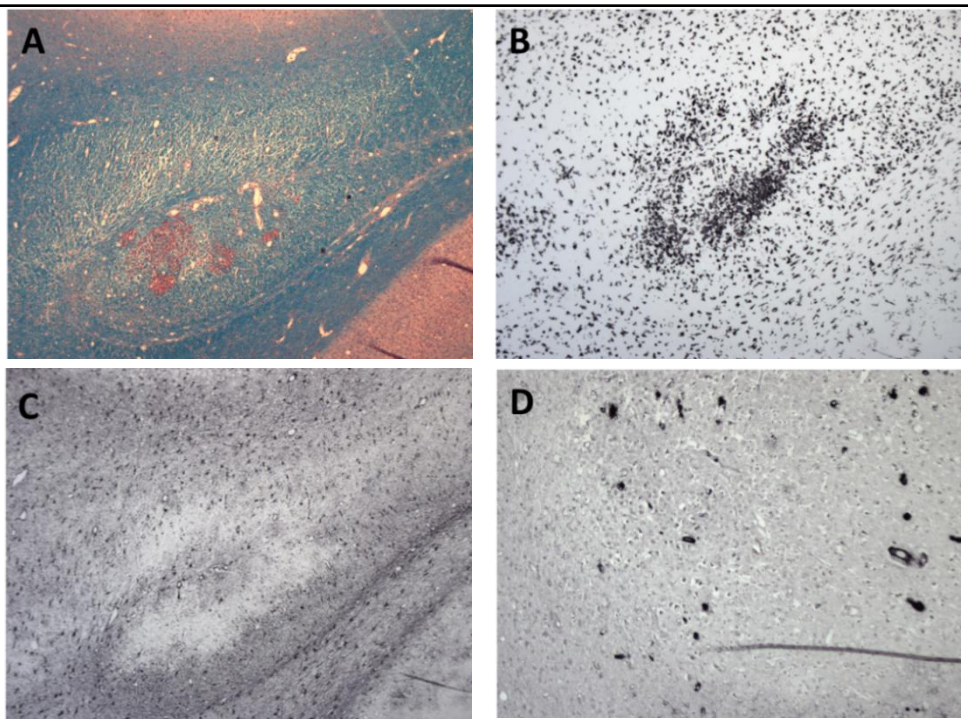

Figure 5A, 5B, 5C, 5D.
Different immunohistochemical procedures were performed to confirm the presence of CAA in the aged SQM model. **5A** shows the usage of Luxol Fast Blue to visualize demyelination, **5B** is a stain of Iba1 for microglia, **5C** shows a stain of GFAP highlighting astrocytes in the brain, and **5D** shows the amyloid that is stained as a result of 6E10/4G8. The visualization and confirmation of these markers helps to further affirm the presence of CAA. (Author)

The confirmation of CAA in the model of SQM was important for the overarching study to correctly affirm that the USPIO-PEG-Aβ nanoparticles were correctly bound to amyloid plaques, and not some other marker. The validation of *Saimiri boliviensis* as an appropriate model for testing of CAA and AD was achieved with the use of cross analysis of ARIA-E evaluation shown in **Figure 4** with the histological work done in **Figure 5**, suggesting that the use of SQMs in future studies for long-term consequences of ARIA and CAA is possible.

3.3 Discussion

The usage of USPIO-PEG-Aβ nanoparticles can help researchers and clinical trials to target and visualize amyloid deposits. The R2* values that were changed suggests that the bi-functional nanoparticle being utilized was accurate in labelling amyloid plaques located in the SQM model. Usage of coregistration and region-of-interest based analysis helped to further the hypothesis that USPIO-PEG-Aβ nanoparticles could correctly label amyloid plaques in the brains of aged SQM. Due to the current difficulty of determining Alzheimer's disease, the ability to do so accurately and in a non-toxic method can prove to be extremely beneficial.

In previous studies, usage of other types of iron oxide particles excluding the binding to a polyethylene glycol molecule had difficulty bypassing the blood-brain barrier (Genovese et al., 2019). Binding the iron oxide nanoparticles to both Aβ and PEG can potentially help future immunotherapeutic studies by providing a basis of accurately determining amyloid burden correlative to CAA. Compared to previous studies dealing with a reliable method of determining severity of Alzheimer's disease, it will now be much easier to determine if treatments are working while animal models are still alive, rather than doing histology after sacrificing the animal subjects (Scholtzova et al., 2016). The USPIO-PEG-Aβ nanoparticles can also be used to monitor plaque burden throughout the course of the disease. This, in turn, may also potentially provide a less invasive and more accurate way of detecting AD, adding to current diagnostic systems such as behavioral tests.

The determination of the aged SQM model for AD pathology, including CAA, will also be important for future human clinical trials on immunotherapeutics and treatments. The aged SQM models were hypothesized to naturally develop CAA pathology (Scholtzova et al., 2015). The confirmation of CAA was done with 6E10/4G8 stains, which aligns with previous research, in which CAA was shown to confirm 6E10. (**Figures 4 and 5**)

Since many immunotherapeutic trials have seen an increase in ARIA pathology during treatment, it was important to find a model that could be monitored throughout the course of a study while still alive (Genovese et al., 2019). The performed immunohistochemical evaluations highlighted specific proteins and markers that were indicative of CAA and astrogliosis (**Figure 5**). The positive results that histological

analyses have shown, especially with its alignment to the ARIA-E noticed in both the FLAIR and RARE scans, helps to postulate that the usage of the aged SQM model for AD and CAA can be potentially useful for future research.

4.0 Conclusion

The non-human primate model of AD pathology is important for translation of medicines to human clinical trials. The confirmation of aged squirrel monkeys as a model for Alzheimer's Disease gives rise to the potential of a precursor prototype of AD immunotherapeutics prior to human clinical trials. The usage of R2* values obtained from region-of-interest based analysis has shown that the post-contrast injection MRI analyses labels the plaques with bi-functional iron oxide nanoparticles. This may be further used by doctors and researchers in the medical field to assess the presence of AD in patients. In addition, the usage of USPIO-PEG-Aβ can be used to continually monitor amyloid plaque burden throughout the course of a study, rather than creating cohorts to be sacrificed at different timepoints to check the efficacy of different immunotherapeutic drugs.

ARIA-E evaluations have also been extremely helpful for the validation of brain vasculature, which can be used in the future for determining the safety for immunotherapeutic approaches. ARIA shows up in every immunotherapeutic trial, where every patient/model develops CAA that shows adverse effects. Not only will this aid the medical field in accurately detecting CAA pathology indicative of AD, but it will also help researchers to more efficiently and accurately detect CAA/AD pathology in models of CAA such as the non-human primate model of aged SQMs.

In addition to the usage of USPIO-PEG-Aβ contrast injections, it was necessary to also assess whether the model of non-human primate model SQMs was effective for modelling AD. The histology that was aligned to amyloid-related imaging abnormalities helped to determine that the SQMs in this study and project was effective.

Given more time to work on this project, I would do immunohistochemical analyses on the USPIO-PEG-Aβ contrast injections. This would help to further affirm that the regions of the brain that the compound labelled were full of biomarkers indicative of CAA. In addition, I would also perform *in vivo* MRI analyses with the USPIOs to determine more accurately that the USPIOs were staining the hypothesized regions. Additional trials and tests would need to be done to further establish the USPIO-PEG-Aβ compound as an accurate indicator of CAA.

5.0 Future Work and Applications

The USPIO-PEG-Aβ nanoparticle contrast injection shows great promise for the use in the field of neuroscience and study of Alzheimer's disease. Due to the current difficulty to accurately determine

whether a form of neurodegeneration in patients is actually Alzheimer's Disease, there is a need for a novel method of detecting amyloid plaques and cerebral amyloid angiopathy that is a pathology of Alzheimer's disease. With the work done to establish USPIO-PEG-Aβ nanoparticles as an effective compound of labeling CAA pathology, it can be used in future studies of a variety of animal models to more accurately determine if the immunotherapies being tested are effective.

The continued usage of ARIA-E evaluation and white matter hyperintensity analysis can be used more in the future to further the research on Alzheimer's disease as well. The ability to confirm the presence of CAA and AD pathology can be confirmed using histological procedures that label markers such as 6E10/4G8 and demyelinated strands, allowing for a more intensive and accurate evaluation of AD pathology in different animal models. This in turn can be used for future clinical trials in various forms of amyloid plaque pathology, specifically with Alzheimer's disease. Further usage of ARIA-E evaluation and MRI analysis with USPIO-PEG-Aβ scans will allow for great affirmation of the compound as a non-toxic and accurate method of detecting amyloidosis in SQMs, and eventually human models.

References

(2019). "Alzheimer's Disease Fact Sheet." Retrieved November 13, 2019, from http://mdanderson.libanswers.com/faq/26219.

Adalbert, R., et al. (2007). "Aβ, tau and ApoE4 in Alzheimer's disease: the axonal connection." Trends in molecular medicine **13**(4): 135-142.

Belaidi, A. A. and A. I. Bush (2016). "Iron neurochemistry in Alzheimer's disease and Parkinson's disease: targets for therapeutics." Journal of neurochemistry **139**: 179-197.

Chan, P., et al. (2019). "Characteristics and effectiveness of cognitive behavioral therapy for older adults living in residential care: a systematic review." Aging & Mental Health: 1-19.

Dong, Y.-X., et al. (2018). "Association between Alzheimer's disease pathogenesis and early demyelination and oligodendrocyte dysfunction." Neural regeneration research **13**(5): 908.

Genovese, T. S., et al. (2019). "NEUROIMAGING AND NEUROPATHOLOGY IN AN AGED NON-HUMAN PRIMATE MODEL OF SPORADIC CAA." Alzheimer's & Dementia: The Journal of the Alzheimer's Association **15**(7): P370.

Gurol, M. E., et al. (2016). "Florbetapir-PET to diagnose cerebral amyloid angiopathy: a prospective study." Neurology **87**(19): 2043-2049.

Korolev, I. O. (2014). "Alzheimer's disease: a clinical and basic science review." Medical Student Research Journal **4**: 24-33.

Lloret, A., et al. (2019). "When Does Alzheimer′ s Disease Really Start? The Role of Biomarkers." International Journal of Molecular Sciences **20**(22): 5536.

Pansieri, J., et al. (2018). "Magnetic nanoparticles applications for amyloidosis study and detection: A review." Nanomaterials **8**(9): 740.

Punia, K., et al. (2019). "Engineered Protein-Iron Oxide Hybrid Biomaterial as Magnetic Imaging-traceable Drug Delivery." IWMPI.

Ruff, J., et al. (2017). "The effects of gold nanoparticles functionalized with ß-amyloid specific peptides on an in vitro model of blood–brain barrier." Nanomedicine: Nanotechnology, Biology and Medicine **13**(5): 1645-1652.

Scholtzova, H., et al. (2014). "Amyloid β and Tau Alzheimer's disease related pathology is reduced by Toll-like receptor 9 stimulation." Acta neuropathologica communications **2**(1): 101.

Scholtzova, H., et al. (2016). "Innate immunity stimulation via Toll-like Receptor 9 as a novel therapeutic approach in Alzheimer's disease." Alzheimer's & Dementia: The Journal of the Alzheimer's Association **12**(7): P1021-P1022.

Scholtzova, H., et al. (2015). "Toll-like receptor 9 stimulation via CpG ODN in a non-human primate model of sporadic cerebral amyloid angiopathy." Alzheimer's & Dementia: The Journal of the Alzheimer's Association **11**(7): P618.

Scholtzova, H., et al. (2018). "INNATE IMMUNITY STIMULATION VIA CLASS C CPG ODN AND MRI MONITORING OF EFFICACY AND SAFETY IN AN AGED NON-HUMAN PRIMATE MODEL OF CAA." Alzheimer's & Dementia: The Journal of the Alzheimer's Association **14**(7): P309.

Scholtzova, H., et al. (2008). "Memantine leads to behavioral improvement and amyloid reduction in Alzheimer's-disease-model transgenic mice shown as by micromagnetic resonance imaging." J Neurosci Res **86**(12): 2784-2791.

Scholtzova, H., et al. (2013). "Innate immunity stimulation via TLR9 in a non-human primate model of sporadic cerebral amyloid angiopathy." Alzheimer's & Dementia: The Journal of the Alzheimer's Association **9**(4): P508.

Wadghiri, Y. Z., et al. (2003). "Detection of Alzheimer's amyloid in transgenic mice using magnetic resonance microimaging." Magnetic Resonance in Medicine: An Official Journal of the International Society for Magnetic Resonance in Medicine **50**(2): 293-302.

Wang, C.-Y., et al. (2010). "Zinc overload enhances APP cleavage and Aβ deposition in the Alzheimer mouse brain." PloS one **5**(12): e15349.

Weissleder, R., et al. (1990). "Ultrasmall superparamagnetic iron oxide: characterization of a new class of contrast agents for MR imaging." Radiology **175**(2): 489-493.

Zhao, Y. and W. J. Lukiw (2015). "Microbiome-generated amyloid and potential impact on amyloidogenesis in Alzheimer's disease (AD)." Journal of nature and science **1**(7).